*ВІСНИК ЛЬВІВ. УН-ТУ*
*Серія фіз. 2009. Вип. 43. С. 199–208*

*VISNYK LVIV UNIV.*
*Ser. Physics. 2009. Is. 43. P. 199–208*

**УДК** 53.083.98
**PACS number(s):** 07.85.Nc, 07.07.Df

# COMBINED XRD, XPS AND PALS CHARACTERIZATION OF HUMIDITY SENSITIVE $MgAl_2O_4$ CERAMICS

**O. Shpotyuk[1], J. Filipecki[2], H. Klym[1,3], A. Ingram[4]**

*[1]Lviv Institute of Materials of SRC "Carat"*
*202, Stryjska Str., 79031 Lviv, Ukraine*
*e-mail: shpotyuk@novas.lviv.ua*
*[2]Institute of Physics of Jan Dlugosz University*
*13/15, al. Armii Krajowej, 42201 Czestochowa, Poland*
*[3]Lviv Polytechnic National University*
*12, Bandera Str., 79013 Lviv, Ukraine*
*[4]Opole University of Technology*
*75, Ozimska Str., 45370 Opole, Poland*

Nanoporous spinel-type $MgAl_2O_4$ ceramics are studied using combined X-ray diffractomentry, high-resolution X-ray photoelectron spectroscopy and positron annihilation lifetime spectroscopy methods. It is shown that microstructure of these ceramics is improved with increase of sintering temperature which mainly results in decreasing of amount of additional phases located near intergranual boundaries. These phase extractions serve as specific trapping centers for positrons penetrating ceramics.

*Key words:* nanopores, spinel, positron trapping, spectroscopy.

Nanoporous magnesium aluminate $MgAl_2O_4$ ceramics with a spinel structure are known to be one of the most perspective materials for environment humidity sensors [1–3]. It is established that sensing functionality of these humidity-sensitive ceramics is determined by microstructure concerning mainly on their phase composition being dependent on ceramics sintering route [4]. With this in mind, the influence of the sintering temperature on the chemical interphase transitions should be studied carefully.

The chemical phase composition of ceramics are known to be typically tested with conventional X-ray diffractomentry (XRD) [5, 6]. Alternative probes such as high-resolution X-ray photoelectron spectroscopy (XPS) can be used for this purpose too. This method allows study chemical states of elements in ceramics [7–9], but being applied to transition-metal spinel compounds it leads to some complications in the developed interpretations because of slightly-resolved features for close cation-related reflexes.

In order to obtain more reliable information on microstructure of $MgAl_2O_4$ ceramics, the developed approach should be based on new additional methods of structural characterization, which allows independent data on phase composition within ceramics bulk. One of them is positron annihilation lifetime spectroscopy (PALS)

[10, 11], the well-known experimental technique to study extended defects in solids despite their structural hierarchy [12].

In this work, we investigate chemical interphase transitions in magnesium aluminate ceramics using XRD, XPS and PALS methods.

The studied ceramics were sintered from fine-dispersive powders of MgO and $Al_2O_3$ oxides at maximal temperature of 1 100–1 400°C during 2 h [11] within conventional ceramics technology route [13]. The phase composition of $MgAl_2O_4$ ceramics was determined by XRD method. The XRD patterns were recorded at room temperature using HZG-4a powder diffractometer with Cu$K\alpha$ radiation. This equipment was attested with NIST SRM-1976 and Si standards. The measurements were carried out in $2u$ step of 0,05° with variable scanning rate, depending on sample quality. The profile analyses were performed using the method of approximation of X-ray reflections by pseudo-Voigt function. The lattice parameters and crystal structures of phases were refined using the Rietveld method with FULLPROF.2k program [14] from WinPLOTR software [15, 16].

The XPS measurements were performed for ceramics sintered at 1 200 and 1 400°C using high-resolution Scienta ESCA–300 spectrometer with monochromatic Al $K_6$ X-rays (1486,6 eV) [17]. To eliminate surface contamination from reaction with atmosphere, the bulk ceramic samples were fractured with a hard tool in ultra-high vacuum inside spectrometer. The XPS data were consist of survey scans over the entire binding energy range and selected scans over core-level photoelectron peaks of interest. An energy increment of 0,05 eV was used for recording the core-level spectra. The core-level peaks were recorded by sweeping the retarding field and using the constant pass energy of 150 eV. The reproducibility of the measurements was checked on different regions of fractured surfaces of a sample. The surface charging from photoelectron emission was neutralized using low energy (< 10 eV) electron flood gun minimizing any distortion and shift of spectra.

The data analysis was conducted with standard ESCA–300 software package. For analyzing core-level spectra, the Shirley background was subtracted and a Voigt line-shape was assumed for all peaks. The concentrations of elements were determined from the area of core-level peaks taking into account the appropriate sensitivities. The full width at half maximum (FWHM) was assumed to be the same for the peaks. Mix between the Gaussian and Lorentzian in the Voigt function was chosen the same for doublet of a given core-level. Fitting procedure gave asymmetry values close to zero for all peaks. With these constraints the uncertainty in peak position and area of each component were ±0,05 eV and ±2%, respectively.

The PALS measurements were performed with an ORTEC spectrometer using $^{22}Na$ source placed between two sandwiched samples as it was described in more details elsewhere [10, 13, 18, 19]. The obtained spectra were mathematically treated with LT computer program [20], the best results corresponding to three-component fitting. Special testing procedure with a set of standard probe samples of thermally-treated non-defected Ni and Al samples was performed to correctly account for source input and other positron trapping channels in the measured PALS spectra. In general, we used three measured PAL spectra for each investigated pair of samples, the best results being chosen by comparing statistically weighted least-squares deviations between experimental points and theoretical curve. In such a way, we obtained the numerical PALS parameters (positron lifetimes $\tau_1$, $\tau_2$ and $\tau_3$ and intensities $I_1$, $I_2$ and $I_3$) which correspond to annihilation of positrons in the samples of interest.

The positron trapping modes in the sintered $MgAl_2O_4$ ceramics were calculated using a known formalism for two-state positron trapping model [18, 12]:

$$\tau_{av.} = \frac{\tau_1 I_1 + \tau_2 I_2}{I_1 + I_2}, \quad \tau_b = \frac{I_1 + I_2}{\frac{I_1}{\tau_1} + \frac{I_2}{\tau_2}} \text{ and } \kappa_d = \frac{I_2}{I_1}\left(\frac{1}{\tau_b} - \frac{1}{\tau_2}\right), \tag{1}$$

where $\tau_b$ is positron lifetime in defect-free bulk, $\tau_{av.}$ – average positron lifetime, $\kappa_d$ – positron trapping rate of defect.

In addition, the ($\tau_2$ - $\tau_b$) difference was accepted as a size measure for extended free-volume defects where positrons are trapped (in terms of equivalent number of monovacancies), as well as the $\tau_2/\tau_b$ ratio was taken in a direct correlation to the nature of these defects [12, 21].

Our results obtained with XRD method testify that the chemical phase composition of the studied $MgAl_2O_4$ ceramics slightly dependence on their sintering temperature $T_s$. Thus, it was established that ceramics sintering route performed at $T_s$ = 1 100°C is not sufficient for single spinel phase formation, since the corresponding XRD patterns of these ceramics contain three phases: the main spinel-type $MgAl_2O_4$ phase (space group $Fd\bar{3}m$) with lattice parameter $a$=8,0705(4) E and some additives of additional MgO (space group $Fm\bar{3}m$) and $\alpha$-$Al_2O_3$ (space group $R\bar{3}c$) phases (see table 1).

*Table 1*

Phase compositions of $MgAl_2O_4$ ceramics obtained with XDR method

| $T_s$, °C | Phase composition/space group | | | | | |
|---|---|---|---|---|---|---|
| | $MgAl_2O_4/Fd\bar{3}m$ | | $\alpha$-$Al_2O_3/R\bar{3}c$ | | MgO/$Fm\bar{3}m$ | |
| | Lattice parameter, E | Weight fraction, % | Lattice parameter, E | Weight fraction, % | Lattice parameter, E | Weight fraction, % |
| 1100 | $a$=8,0705(4) | 80,62 | $a$=4,7585(4), $c$=12,992(2) | 8,13 | $a$=4,2108(1) | 11,25 |
| 1200 | $a$=8,0796(3) | 88,12 | $a$=4,7585(5), $c$=12,991(2) | 6,06 | $a$=4,2112(2) | 5,82 |
| 1300 | $a$=8,0822(2) | 96,52 | – | – | $a$=4,2114(3) | 3,48 |
| 1400 | $a$=8,0828(1) | 98,46 | – | – | $a$=4,2117(7) | 1,54 |

The ceramics obtained at 1 200°C are three-phase too, but the main spinel with lattice parameter $a$=8,07996(3) E is formed more intensively. In contrast, the ceramics sintered at 1 300 °C contain only two phases, the main spinel-type and MgO phases (the remainders of $\alpha$-$Al_2O_3$ phase disappears). The ceramics sintered at $T_s$=1 400°C in addition to the main spinel phase with lattice parameter $a$=8,0828(1) E have a small quantity of MgO phase in comparison with the ceramics sintered at $T_s$=1 300°C (the corresponding contents of MgO phase in the above ceramics are ~3,5 and 1,5%, respectively) [10, 11].

Thus, increase in the sintering temperature from 1 100 to 1 400°C causes the following reaction of spinel-phase formation, the corresponding lattice parameter a slightly rising within this process being at the level of 8,08 E (see table 1). So we can conclude that in magnesium aluminate ceramics the same spinel-type phase is formed whichever $T_s$.

Survey scans of the studied $MgAl_2O_4$ ceramic samples sintered at 1 200 and 1 400°C and fractured in the ultra-high vacuum of the spectrometer are shown in fig. 1. The peaks associated with the Mg, Al and O core levels of the main spinels, C signal as well as peaks related to Auger lines are identified using the known reference spectra [9]. The well-defined C peak in the survey spectrum on fig. 2 testifies in a favor of incomplete ceramics sintering process or possible adsorption by ceramics surface during XPS measurements. But, like as in [8], this C-related XPS signal does not change significantly the overall results for $MgAl_2O_4$ ceramics.

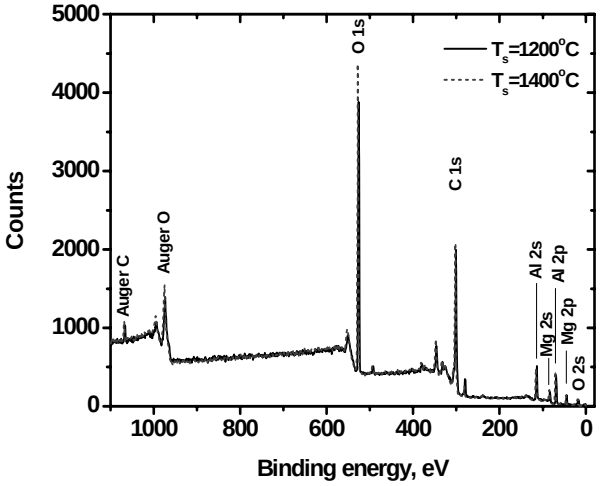


Fig. 1. Survey XPS spectra for $MgAl_2O_4$ ceramics sintered at 1 200 and 1 400°C

The numerical parameters of XPS core-level spectra (Al 2*p*, Mg 2*p* and O 1*s*) of the studied $MgAl_2O_4$ ceramics sintered at 1 200 and 1 400 °C are gathered in table 2. They are in well agreement with typical values given by other authors [5–9].

The Al 2*p* core-level XPS spectrum was deconvoluted into spin-orbit doublet $2p_{3/2}$ and $2p_{1/2}$, whose separation and area ratios were fixed and maintained using the data previously obtained for pure element standards [7]. The parameters used to link Al $2p_{3/2}$ and Al $2p_{1/2}$ peaks were 0,44 eV in peak separation and 0.5 in area ratio. These reference values were obtained experimentally for pure bulk Al using Scienta ESCA–300 spectrometer. The binding energies of this $2p_{3/2}$ and $2p_{1/2}$ doublet are 73**,**5 and 74**,**0 eV, respectively, in full correspondence to the known experimental data [5, 7, 8].

In contrast, the Mg 2*p* core-level XPS spectrum was single type with corresponding binding energy of 49**,**3 eV (the same values is given in [7, 8]).

The O 1*s* core-level spectrum was deconvoluted into two independent peaks, the biggest peak marked as O 1*s*-I with ~530**,**3 eV binding energy and the smaller one marked as O 1*s*-II with binding ~531**,**1–531**,**9 eV energy (see fig. 2 and table 2) corresponding well with known experimental data [7, 8]. Two O 1*s* peaks in the deconvoluted core-level XPS spectra of the studied $MgAl_2O_4$ ceramics testify in a favor of chemically different positions possible for O atoms.

*Table 2*

Numerical parameters of XPS core-level spectra
for $MgAl_2O_4$ ceramics sintered at 1 200 and 1 400°C

| Element/ Transition | $T_s$=1 200 °C | | | $T_s$=1 400 °C | | |
|---|---|---|---|---|---|---|
| | Position, eV | FWHM, eV | Area, % | Position, eV | FWHM, eV | Area, % |
| Mg 2*p* | 49,3 | 1,61 | 100 | 49,3 | 1,57 | 100 |
| Al $2p_{3/2}$ | 73,5 | 1,57 | 67 | 73,5 | 1,47 | 67 |
| Al $2p_{1/2}$ | 74,0 | 1,57 | 33 | 74,0 | 1,47 | 33 |
| O 1*s*-I | 530,3 | 1,75 | 81 | 530,3 | 1,75 | 94 |
| O 1*s*-II | 531,1 | 1,94 | 19 | 531,9 | 1,42 | 6 |

To develop an adequate interpretation of these XPS reflexes, the above presented XRD results were taken as a basic. By accepting that two O 1*s* peaks are observed for the deconvoluted core-level spectra of $MgAl_2O_4$ ceramics sintered at 1 400°C having two phases (see table 1), we can attribute these XPS reflexes to prevailed spinel-type and additional $MgO/Al_2O_3$ phases. Therefore, the O 1*s*-I peak at ~530,3 eV having the highest intensity corresponds to the main spinel-type phase, while the smaller one (O 1*s*-II at ~531,1–531,9 eV) – to the remainders of additional $MgO/Al_2O_3$ phases. In addition, taking into account that crystallographical parameters of the prevailing spinel-type phase is only slightly affected by sintering temperature (see table 1), we can suppose the constant value of FWHM in the deconvolution procedure for the tested ceramics with all changes being reflected in the binding energy of corresponding core-level peaks. In respect to the known previous data [7], we perform the fitting route with FWHM maintained as high as 1,75 eV.

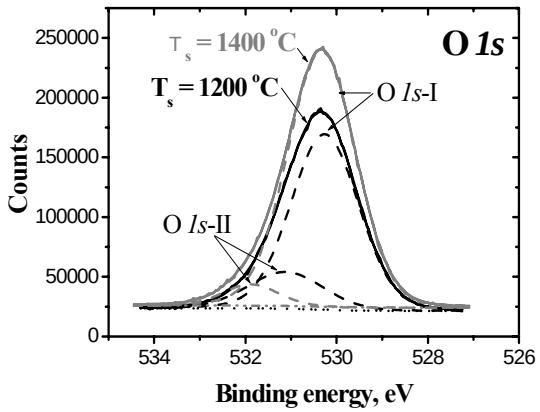


Fig. 2. Peak-normalized PALS spectra for studied $MgAl_2O_4$ ceramics sintered at 1 100–1 400°C

Within this approach, it is obvious that the area and intensity of O 1*s*-I core-level peak increases with sintering temperature in accordance to the content of the main spinel phase in the ceramics (see table 2). Otherwise, the area of O 1*s*-II core-level XPS peak decrease from 19% in ceramics sintered at 1 200°C to 6% for ceramics sintered at 1 400°C.

These changes correspond well to main tendencies in the phase composition of the studied ceramics revealed with XRD. Some discrepancies in the numerical values of phase fractions are probably due to different local sensitivities of the applied techniques.

Within the supposition on constant FWHM value for the main spinel-type phase in the studied ceramics reflected in O 1*s*-I core-level peak, we can treat the FWHM value of the second O 1*s*-II peak as corresponding manifestation for chemical perfectiveness of additional phases. As it testified from Table 2, the greater content of additional phases (transition to ceramics sintered at lower $T_s$) leads to the increase in FWHM (from 1**,**94 to 1**,**42 eV for ceramics sintered at 1 200 and 1 400°C, respectively). This behavior is ruled by a variety of additional phases segregated in the prepared ceramics, since $Al_2O_3$ phase appears in addition to MgO phase.

Thus, the high-resolution XPS method in application to O 1*s* core-level spectrum allows us to identify the chemical states of composing atoms within ceramics bulk. In such a way, we have an additional confirmation on the phase separation effects in the studied ceramics.

In respect to our previous XRD and XPS measurements, the studied $MgAl_2O_4$ ceramics have a different amount of additional $MgO/Al_2O_3$ phases. In accordance with the scanning electron microscopy data presented in [10], the observed additional phases are non-uniformly distributed within ceramics bulk, being more clearly pronounced near intergranual boundaries. These phase extractions serve as specific trapping centers for positrons penetrating ceramics. So by using PALS method in addition to XRD and XPS, we shall try to identify more carefully positron trapping characteristics of these extracted phases in $MgAl_2O_4$ ceramics sintered at different $T_s$.

The normalized PALS spectra of the studied $MgAl_2O_4$ ceramics sintered at 1 100–1 400°C are shown in fig. 3. They are characterized by a narrow peak and region of a long fluent decaying of coincidence counts in a time. The mathematical decay of such curve can be represented by a sum of decreasing exponents with different values of power-like indexes inversed to positron lifetimes [12, 22].

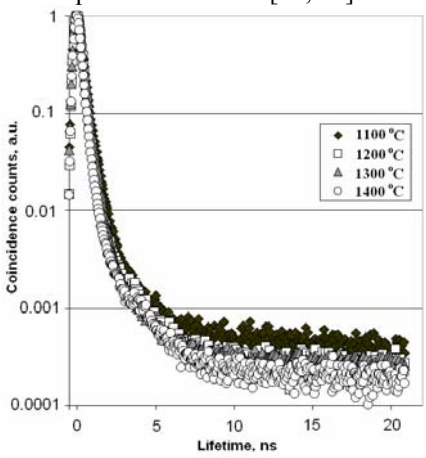


Fig. 3. Peak-normalized PALS spectra for studied $MgAl_2O_4$ ceramics sintered at 1 100–1 400°C

As was shown in [10, 11], in the case of $MgAl_2O_4$ ceramics, two channels of positron annihilation should be considered – the positron trapping with shortest $\tau_1$ and middle $\tau_2$ lifetimes and o-Ps decaying (so-called "pick-off" annihilation) with longest $\tau_3$ lifetime, these channels being independent ones.

Taking into account the model described in [10, 12, 22], the shortest lifetime component (the first channel of positron annihilation) in the studied ceramics reflects mainly the microstructure specificity of the spinel with character octahedral and tetrahedral cation vacancies. It is shown (see table 3) that the lifetime $\tau_1$ and intensity $I_1$ of this first component slightly increase with $T_s$ (see table 1 and table 3). Obviously, the decreasing of $\tau_1$ lifetime reflects more perfect ceramics structure prepared at higher $T_s$.

By accepting two-state positron trapping model [17, 20], the longer $\tau_2$ lifetime can be treated as defect-related one, these positron trapping defects being located near intergranual boundaries [10, 13]. In respect to our XRD measurements, in the studied $MgAl_2O_4$ ceramics, the amount of additional phases is dependent on $T_s$ (see table 1). So the positrons are trapped more strongly in the spinel-type ceramics obtained at lower $T_s$, which is reflected in the middle component of lifetime spectra.

*Table 3*

PALS characteristics of $MgAl_2O_4$ ceramics sintered at 1 100–1 400°C mathematically treated within three-component fitting procedure

| $T_s$, °C | Fitting parameters | | | | | |
|---|---|---|---|---|---|---|
| | $\tau_1$, ns | $I_1$, a.u. | $\tau_2$, ns | $I_2$, a.u. | $\tau_3$, ns | $I_3$, a.u. |
| 1 100 | 0,20 | 0,80 | 0,43 | 0,18 | 2,15 | 0,02 |
| 1 200 | 0,18 | 0,74 | 0,38 | 0,25 | 1,88 | 0,02 |
| 1 300 | 0,17 | 0,75 | 0,36 | 0,23 | 2,14 | 0,02 |
| 1 400 | 0,17 | 0,74 | 0,35 | 0,23 | 1,83 | 0,02 |
| $T_s$, °C | Positron trapping modes | | | | | |
| | $\tau_{av.}$, ns | $\tau_b$, ns | $\kappa_d$, $ns^{-1}$ | $\tau_2 - \tau_b$, ns | $\tau_2/\tau_b$ | |
| 1 100 | 0,25 | 0,23 | 0,5 | 0,21 | 1,9 | |
| 1 200 | 0,23 | 0,20 | 0,7 | 0,20 | 1,9 | |
| 1 300 | 0,22 | 0,20 | 0,7 | 0,16 | 1,9 | |
| 1 400 | 0,21 | 0,19 | 0,7 | 0,16 | 1,9 | |

As it followed from table 3, the fitting parameters of this lifetime component ($\tau_2$ and $I_2$) significantly decrease with $T_s$. Consequently, the corresponding positron trapping modes of extended defects near intergranual boundaries will be changed too. Indeed, the values of such parameters as $\tau_{av.}$, $\tau_b$ and ($\tau_2 - \tau_b$) decrease with $T_s$ in good accordance with amount of additional $MgO/Al_2O_3$ phases in the studied ceramics. But in all cases, the same type of positron trapping centre is formed since there are no differences in $\kappa_d$ and $\tau_2/\tau_b$ values with $T_s$. The character size of these extended positron traps near intergranual boundaries estimated due to ($\tau_2 - \tau_b$) difference is close to single-double atomic vacancies [12].

The third longest component in the resolved lifetime spectra at the level of 1,83–2,15 ns is due to "pick-off" annihilation of o-Ps atoms in the intergranual pores [12]. Despite small $I_3$ intensity (2%), this component cannot be eliminated without significant losses in the goodness of the fitting procedure. The similar component was detected in different porous substances whichever their structural type [22, 24]. It can be surmised this component is owing to predominant o-Ps "pick-off" decaying in the

intergranual nanopores filled with absorbed water [11]. These changes in the lifetime $\tau_3$ are connected with more branched structure of the open pores [24] of the ceramics sintered at higher $T_s$ (1 300 and 1 400°C). In ceramics sintered at 1 400°C, this lifetime closed to 1,83 ns approximating to $\tau_3$ = 1,84 ns value which is character for o-Ps "pick-off" decaying in liquid water [11]. With $T_s$ growing, the o-Ps "pick-off" decaying occurs preferentially in the nanopores filled by absorbed water.

Thus, the obtained PALS results well agree with phase composition study of $MgAl_2O_4$ ceramics with XRD and XPS methods.

The combined using of XPS, XRD and PALS methods is a quite informative tool to study chemical phase interactions in spinel-type magnesium aluminate $MgAl_2O_4$ ceramics caused by their technological modification owing to sintering temperature $T_s$.

The authors thank Dr. P. Demchenko (Ivan Franko National University of Lviv, Ukraine) for XRD measurements and Prof. H. Jain (Lehigh University, PA, Bethlehem, USA) for XPS measurements.

1. *Traversa E.* Ceramic sensors for humidity detection: the state-of-the-art and future developments // Sens. and Actuat. 1995. Vol. B. 23. P. 135–156.
2. *Gusmano G., Montesperelli G. , Traversa E.* Microstructure and electrical properties of $MgAl_2O_4$ thin film for humidity sensors // J. Am. Ceram. Soc. 1993. Vol. 76. P. 743–750.
3. *Gusmano G., Montesperelli G., Traversa E.* et al. Magnesium aluminate spinel thin film as a humidity sensor // Sens. and Actuat. B. 1992. Vol. 7. P. 460–463.
4. *Seiyama T., Yamazoe N., Arai H.* Ceramic humidity sensors // Sens. and Actuat. 1983. Vol. 4. P. 85–96.
5. *Asami K., Mitani S., Fujimori H., Ohnuma S., Masumoto T.* Characterization of Co-Al-O magnetic thin films by combined use of XPS, XRD and EPMA // Surf. Interface Anal. 1999. Vol. 28. P. 250–253.
6. *Asami K., Ohnuma T.* XPS and X-ray diffraction characterization of thin Co-Al-N alloy films prepared by reactive sputtering deposition // Surf. Interface Anal. 1998. Vol. 26. P.659–666.
7. Briggs D., Sean M.P. Practical surface analysis. Auger and X-ray photoelectron spectroscopy. England. 1996. 483 p.
8. *Strohmeier B.R.* Magnesium aluminate ($MgAl_2O_4$) by XPS // Surf. Sci. Spectra. 1995. Vol. 3. P. 121–127.
9. *Moulder F., Stickle W.F., Sobol P.E., Bomben K.D.* Handbook of X-ray Photoelectron Spectroscopy. ed. J. Chastein. Perkin-Elmer Corp. Phys. Electr. Div. Eden Prairie : Minnesota. 1992.
10. *Balitska V., Filipecki J., Ingram A., Shpotyuk O.* Defect characterization methodology in sintered functional spinels with PALS technique // Phys. Stat. Sol. (C). 2007. Vol. 4. No 3. P. 1317–1320.
11. *Klym H., Ingram A., Shpotyuk O., Filipecki J.* et al. Extended positron-trapping defects in insulating $MgAl_2O_4$ spinel-type ceramics // Phys. Stat. Sol. (C). 2007. Vol. 4. No 3. P. 715–718.
12. *Krause-Rehberg R., Leipner H.S.* Positron annihilation in semiconductors. Defect Studies, Springer-Verlag: Berlin-Heidelberg-New York. 1999. 378 p.

13. *Shpotyuk O., Ingram A., Klym H.* et al. PAL spectroscopy in application to humidity-sensitive $MgAl_2O_4$ ceramics // J. Europ. Ceram. Soc. 2005. Vol. 25. P. 2981–2984.
14. *Rodriguez-Carvajal J.* Recent developments of the program FULLPROF. Commission on Powder Diffraction (IUCr) // Newsletter. 2001. Vol. 26. P. 12–19.
15. *Roisnel T., Rodriguez-Carvajal J.* WinPLOTR: a windows tool for powder diffraction patterns analysis. Materials Science Forum // Proc. of the Seventh European Powder Diffraction Conference, Barcelona. 2000. P. 118–123.
16. *Hill R.J., Howard C.J.* Quantitative phase analysis from neutron powder diffraction data using the Rietveld method // J. Appl. Cryst. 1987. Vol. 20. P. 467–474.
17. *Shpotyuk O., Kovalskiy A., Golovchak R.* et al. Radiation-induced defects in chalcogenide glasses characterizaed by combined optical spectroscopy, XPS and PALS methods // Phys. Stat. Sol. (C). 2006. Vol. 4. N 3. P. 131–134.
18. *Shpotyuk O., Filipecki J.* Free volume in vitreous chalcogenide semiconductors: possibilities of positron annihilation lifetime study. Czestochowa: 2003. 114 p.
19. *Shpotyuk O., Kovalskiy A., Filipecki J., Kavetskyy T.* Positron annihilation lifetime spectroscopy as experimental probe of free volume concepts in network glasses // Phys. Chem. Glasses: Eur. J. Technol. B. 2006. Vol. 47. N 2. P. 131–135.
20. *Kansy J.* Positronium trapping in free volume of polymers. Rad. Phys. Chem. 2000. Vol. 58. P. 427–431.
21. *Nambissan P.M.G.., Upadhyay C., Verma H.C.* Positron lifetime spectroscopic studied of nanocrystalline $ZnFe_2O_4$ // J. Appl. Phys. 2003. Vol. 93. P. 6320–6326.
22. *Bigg D.M.* A review of positron annihilation lifetime spectroscopy as applied to the physical ageing of polymers // Polym. Engin. and Sci. 1996. Vol. 36. N 6. P. 737–734.
23. *Ghosh S., Nambissan P.M.G., Bhattacharya R.* Positron annihilation and Mцssbauer spectroscopic studies of $In^{3+}$ substitution effects in bulk and nanocrystaline $MgMn_{0.1}Fe_{1.9-x}O_4$ // Phys. Lett. A. 2004. Vol. 325. P. 301–308.
24. *Elssner G., Hoven H., Kiessler G., Wellner P.* Ceramics and ceramic composites: Materialographic preparation. Elsevier. 1999. 73 p.

## ДОСЛІДЖЕННЯ ВОЛОГОЧУТЛИВОЇ КЕРАМІКИ $MgAl_2O_4$ КОМБІНОВАНИМИ МЕТОДАМИ РДМ, РФЕС ТА ПАС

**О. Шпотюк[1], Я. Філіпецький[2], Г. Клим[1,3], А. Інграм[4]**

*[1]Науково-виробниче підприємство "Карат"*
*вул. Стрийська 202, 79031 Львів, Україна*
*[2]Інститут фізики, Ууніверситету Яна Длугоша*
*вул. Армії Крайової 13/15, 42201 Ченстохова, Республіка Польща*
*[3]Національний університет "Львівська політехніка"*
*вул. Бандери 12, 79013 Львів, Україна*
*[4]Опольський технічний університет*
*вул. Озімска 75, 45370 Ополє, Республіка Польща*

Досліджено нанопорувату шпінельну кераміку $MgAl_2O_4$ з використанням комбінованих методів рентгенівської дифрактометрії, високороздільної рентге-

нівської фотоелектронної спектроскопії та позитронної анігіляційної спектроскопії. Показано, що мікроструктура цієї кераміки визначається температурою, яка призводить до зменшення вмісту додаткових фаз поблизу меж зерен. Ці виділені фази слугують центрами захоплення позитронів у кераміці.

*Ключові слова:* нанопори, шпінель, захоплення позитронів, спектроскопія.

## ИССЛЕДОВАНИЕ ВЛАГОЧУВСТВИТЕЛЬНОЙ КЕРАМИКИ $MgAl_2O_4$ КОМБИНИРОВАННЫМИ МЕТОДАМИ РДМ, РФЭС И ПАС

**О. Шпотюк[1], Я. Филипецкий[2], Г. Клим[1,3], А. Инграм[4]**

*[1]Научно-производственное предприятие "Карат"*
*ул. Стрыйская 202, 79031 Львов, Украина*
*[2]Институт физики, Университет Яна Длугоша*
*ул. Армии Краевой 13/15, 42201 Ченстохова, Республика Польша*
*[3]Национальний университет "Львовская политехника"*
*ул. Бандеры 12, 79013 Львов, Украина*
*[4]Опольский технический университет*
*ул. Озимска 75, 45370 Ополе, Республика Польша*

Исследовано нанопористую шпинельную керамику $MgAl_2O_4$ с использованием комбинированных методов рентгеновской дифрактометрии, высокораздельной рентгеновской фотоэлектронной спектроскопии и позитронной аннигиляционной спектроскопии. Показано, что микроструктура этой керамики определяется температурой, которая приводит к уменьшению содержания дополнительных фаз вблизи пределов зерен. Эти выделенные фазы служат центрами захвата позитронов в этой керамике.

*Ключевые слова:* нанопоры, шпинель, захват позитронов, спектроскопия.

Стаття надійшла до редколегії 04.06.2008
Прийнята до друку 25.03.2009